RSC Advances

PAPER

View Article Online
View Journal | View Issue

Cite this: *RSC Adv.*, 2019, **9**, 668

Role of the disulfide bond on the structure and activity of μ-conotoxin PIIIA in the inhibition of $Na_V1.4$†

Xiaoxiao Xu,[ab] Qingliang Xu,[ab] Fangling Chen,[ab] Juan Shi,[ab] Yuntian Liu,[ab] Yanyan Chu,[b] Shengbiao Wan,[ab] Tao Jiang[ab] and Rilei Yu*[ab]

Received 19th July 2018
Accepted 23rd October 2018

DOI: 10.1039/c8ra06103c

rsc.li/rsc-advances

μ-Conotoxin PIIIA, a peptide toxin isolated from *Conus purpurascens*, blocks the skeletal muscle voltage-gated sodium channel $Na_V1.4$ with significant potency. PIIIA has three disulfide bonds, which contribute largely to its highly constrained and stable structure. In this study, a combination of experimental studies and computational modeling were performed to assess the effects of deletion of the disulfide bonds on the structure and activity of PIIIA. The final results indicate that the three disulfide bonds of PIIIA are required to produce the effective inhibition of $Na_V1.4$, and the removal of any one of the disulfide bonds significantly reduces its binding affinity owing to secondary structure variation, among which the Cys11–Cys22 is the most important for sustaining the structure and activity of PIIIA.

1. Introduction

Voltage-gated sodium channels (VGSCs) are responsible for the initiation and propagation of action potentials in many organs from the nervous system to the heart and muscles.[1–3] μ-Conotoxins, members of the M superfamily,[4,5] contain 16 to 25 residues with six Cys residues arranged in a class III framework (–C1C2–C3–C4–C5C6–)[6] and are considered to be specific antagonists of voltage-gated Na^+ channels.[7] The μ-conotoxin PIIIA was isolated from *Conus purpurascens*, an eastern Pacific fish hunting species of cone snails.[8] It is a 22-amino acid peptide, consisting of six cysteines and forming three pairs of disulfide bonds.[9] The μ-conotoxins PIIIA and GIIIA are both high-affinity antagonists with skeletal muscle Na channel subtypes from a variety of vertebrate system, and PIIIA is also an irreversible inhibitor in the amphibian system.[10] PIIIA selectively inhibits the skeletal muscle channel $Na_V1.4$ with a half-maximal inhibitory concentration (IC_{50}) value in the nanomolar range (36 nM),[8] and can also block $rNa_V1.2$ and $rNa_V1.7$ at IC_{50} values of 690 nM and 6.2 μm, respectively (Fig. 1).[11] Hence, it is valuable for use as a probe to enable different subtypes to be distinguished when used in conjunction with other selective toxins.[11,12] In addition, PIIIA can also inhibit the $K_V1.1$ and $K_V1.6$ channels in the nanomolar range.[13]

Related studies have shown that the disulfide connectivity alters the global fold of a toxin.[14] Disulfide bonds in the peptide sequence give rise to a well-defined and constrained framework and generally play an important role in their biological action,[15] but this also present challenges. The most critical step for the preparation of disulfide-bridged conopeptides is the oxidation to the correctly folded isomer[16] and a related study has shown that the disulfide-bridges are susceptible to reduction in certain extracellular environments such as the blood.[17] Thus, simplifying the disulfide bonds in peptides is of paramount importance for the application of peptides in pharmacy and other fields. Indeed, growing evidence suggests that many disulfide-rich peptides do not require all their native disulfide bonds to retain their biological activity.[18,19] For instance, removal of the Cys1–Cys16 bridge in ω-conotoxin MVIIA does not abolish its calcium channel binding affinity.[20] Some results have also shown that the key residues of KIIIA for voltage-gated sodium channel (VGSC) binding lie mostly on the alpha-helix and that the first disulfide bond can be removed without significantly affecting the structure of this helix, and its biological activity.[21] This is not only isolate to the native peptide, removal of one of the disulfide bonds in the backbone cyclized Vc1.1 (cVc1.1) produced hcVc1.1, which maintained the secondary structure of the cVc1.1 and showed only a threefold decrease in the activity.[22] Thus, it is possible to maintain the structure and activity of the peptide by the deletion of one of the disulfide bonds.

In this study, the contribution for each of the disulfide bonds to the structure and activity of the PIIIA was investigated by

[a]*Key Laboratory of Marine Drugs, Chinese Ministry of Education, School of Medicine and Pharmacy, Ocean University of China, Qingdao, 266003, China. E-mail: ryu@ouc.edu.cn; Tel: +86-138-6986-2306*

[b]*Laboratory for Marine Drugs and Bioproducts of Qingdao National Laboratory for Marine Science and Technology, Qingdao 266003, China*

† Electronic supplementary information (ESI) available. See DOI: 10.1039/c8ra06103c

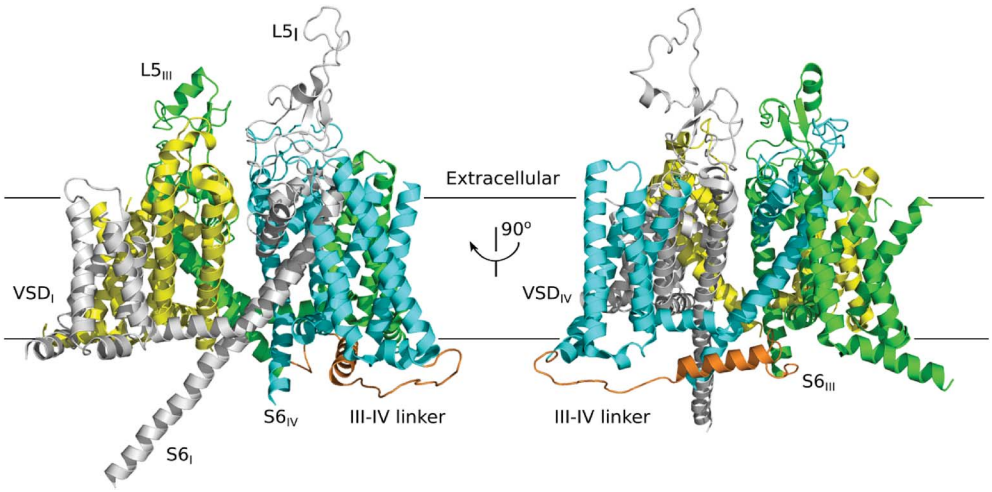

Fig. 1 Electron microscopy structure of the $Na_V1.4$ of eukaryotic (PDB ID: 5XSY). The Na_V α subunits have the same topological structure, and the single polypeptide chain folds into four repeats represented in blue, gray, yellow and green, each containing six transmembrane segments (TMs) (S1–S6). This $Na_V1.4$ consists of the extracellular domain and the VSD (voltage sensing domain).

a combination of experimental studies and computational modeling. The produced results could be used as guidance for further engineering of the structure of PIIIA in future studies.

2. Materials and methods

2.1 Chemical synthesis of the peptides

The peptides were synthesized using a 9-fluorenylmethoxycarbonyl (Fmoc) solid phase peptide synthesis (SPPS) as described previously.[23] The substitution of pyroglutamic with alanine does not affect the inhibitory activity as illustrated by the fact that the pyroglutamic acid plays a minor role in the binding between the PIIIA and $Na_V1.4$.[24] Thus, it is feasible to replace the pyroglutamic acid with another amino acid. In consideration of the structural similarity between pyroglutamic acid and proline, proline was used to replace the pyroglutamic acid to give minimal structure perturbation. The four cysteine residues in the disulfide deleted analogues were protected by using trityl and Acm groups for the selective oxidation. A two-step oxidation protocol was used to selectively fold the peptides. The first disulfide bond was oxidized in 0.1 M NH_4HCO_3 (pH 8–8.5) at a peptide concentration of 0.3 mg mL^{-1} with stirring for 24 h at room temperature. Afterward, the products were purified using reversed-phase high performance liquid chromatography (RP-HPLC) on a Phenomenex C_{18} column (250 × 10 mm, 10 μm).

Formation of the second disulfide bond was performed by dissolving 10 mg peptide in 10 mL (c = 0.42 mM) buffer A/B (Table S1†), and adding 0.2 mL I_2 solution dropwise (5 mg I_2 dissolved in 1 mL CH_3CN) with stirring for 30 min, then quenching with ascorbic acid (5 mg ascorbic acid dissolved in 1 mL H_2O). After the oxidation, the products were purified using RP-HPLC. After confirming the product peak using mass spectrometry, the solid peptide was obtained by lyophilization. Analytical RP-HPLC with a gradient of 0–80% buffer B (the specific concentration ratio is shown in Table S1†) and a flow rate of 1 mL min^{-1} in 40 min and electrospray-mass spectroscopy was used to confirm the purity and molecular mass of the synthesized peptides (Fig. S1 and Table S4†).

2.2 Circular dichroism spectra

The circular dichroism (CD) spectra of PIIIA* and its analogues were performed on a Jasco J-810 spectropolarimeter over the wavelength range of 250–190 nm using a 1.0 mm path length cell, a bandwidth of 1.0 nm, a response time of 2 s, and the results were averaged over three scans. The spectra were recorded at room temperature under a nitrogen atmosphere. A blank scan was performed before the analysis of the samples was performed. The peptides were dissolved with buffer A or B (Table S1†), reaching a concentration of 0.1 mmol L^{-1}. The quality of each peptide can be found in Table S2.† The molar ellipticity $[\theta]$ were fitted with linear regression using the following equation:

$$[\theta] = 1000\text{mdeg}/(l \times C)$$

In which mdeg represents the raw CD data, C represents the peptide molar concentration (mM), and l represents the cell path length (mm).

2.3 Electrophysiology

Whole-cell patch-clamp recordings from HEK293 cells were performed using an Axon digidata 1550A amplifier. The α subunit of the $Na_V1.4$ oocytes was prepared and a double electrode voltage clamp was used for recording. Similar to previous studies,[25–31] the cells were perfused with extracellular solution containing 137 mM NaCl, 4 mM KCl, 1.8 mM $CaCl_2$, 1 mM $MgCl_2$, 10 mM HEPES, and 10 mM glucose. The pH of the solution was adjusted to 7.4 using NaOH. The oocytes were placed in a vial containing 30 μL ND96 and two electrodes voltage clamped in the −80 mV holding potential chamber, repeating every 10 seconds, each time with 10 millisecond

square wave membrane potential depolarized to −10 mV, to activate the $Na_V1.4$ ion channel current. The maximum current caused by the voltage-clamp square wave was detected and the compound was tested by perfusion after being stabilized. The compounds were dissolved in extracellular fluid and perfused using a self-gravity perfusion system. Extracellular fluid containing 130 mM Cs aspartate, 5 mM $MgCl_2$, 5 mM EGTA, 10 mM HEPES and 4 mM Tris-ATP was used with the pH adjusted to 7.2 by addition of CsOH. The test concentrations of the peptides were set at 0.1, 0.3, 1, 1, 3, and 10 μm (Table S3†), respectively. At least two cells were tested at each concentration. After the current caused by the voltage clamp square wave was stabilized, the changes in the current size before and after the use of the peptide were compared and the blocking effects of the peptide on the $Na_V1.4$ channels was calculated.

2.4 Homology modeling

The NMR structure of PIIIA (PDB code: 1R9I) was obtained from the protein data bank (http://www.rcsb.org/). PIIIA* and its three analogues, each with one different pair of disulfide-bonded cysteine residues replaced with alanine, were constructed as shown in Table 1. The three disulfide bonds (Cys4–Cys16, Cys5–Cys21, and Cys11–Cys22) of PIIIA* were numbered as 1, 2 and 3, respectively, and the corresponding disulfide deleted analogues were named as PIIIA*-x ($x = 1, 2, 3$), in which each number represents that the corresponding disulfide bond that was removed. PIIIA*-1, PIIIA*-2, and PIIIA*-3 were constructed in MODELLER (version 9v16),[32,33] as described previously.[34] PIIIA* and its analogues was subjected to further refinement of the molecular dynamics (MD) simulations.

2.5 Molecular dynamics simulation

By modifying the model we built and validated previously,[35] we obtained the complexes: $Na_V1.4$/PIIIA*-1, $Na_V1.4$/PIIIA*-2, and $Na_V1.4$/PIIIA*-3. These complexes were subjected to MD simulations for refinement of the PIIIA* binding mode in AMBER 16.[36] After building the whole system in LEaP, a module of AMBER16, minimization was performed to remove the van der Waals clashes between PIIIA* and $Na_V1.4$. Other details regarding the methods used for MD simulation are described in our previous study.[37] PIIIA* and its analogues were refined using 100 ns MD simulations, while the complexes were refined using 20 ns MD simulations. The last conformation was extracted from the MD trajectory.

Table 1 Sequence of μ-conotoxins PIIIA and its analogues[a]

Peptide	Name	Sequence
PIIIA	PIIIA	PCA RLCCGFOKSCRSRQCKOHRCC
PIIIA*	PIIIA*	PRLCCGFOKSCRSRQCKOHRCC
PIIIA*-1	PIIIA*[C4A,C16A]	PRLACGFOKSCRSRQAKOHRCC
PIIIA*-2	PIIIA*[C5A,C21A]	PRLCAGFOKSCRSRQCKOHRAC
PIIIA*-3	PIIIA*[C11A,C22A]	PRLCCGFOKSARSRQCKOHRCA

[a] PIIIA* is an analogue of PIIIA in which the first amino acid is replaced using Pro. PIIIA*-1, 2, 3 represents the analogue missing the first (Cys4–Cys16), second (Cys5–Cys21) and third (Cys11–Cys22) disulfide bond, respectively.

2.6 Binding energy calculations using MMGB/SA

A molecular mechanics generalized Born surface area (MMGB/SA)[38] was applied to calculate the energy contributed by the key amino acids of the peptide. For efficient conformation sampling, the binding energy calculation was performed on the five MD trajectories using MMGB/SA and the averaged values were used as the final result. The parameters used for setting up were the same as those previously described.[34]

3. Results and discussion

3.1 Chemical synthesis of peptides

After the solid phase reaction had finished, half of the resin peptide was partially deprotected and cleaved from the resin with TFA. For PIIIA*-1, the protecting group of Cys5 and Cys21 is trityl (trt), while the protecting group of Cys11 and Cys22 is acetamidomethyl (Acm). The trt protection group of Cys5 and Cys21 can be deprotected in a mixture of TFA/TIS/H_2O (90 : 5 : 5), whereas the Acm protection group can only be removed in I_2 solvent. Thus, in the first round oxidation in NH_4HCO_3, only the disulfide bond Cys5–Cys21 was formed, whereas the second disulfide bond Cys11–Cys22 was formed during the oxidation using I_2 solvent. The product of each step was obtained by purification using RP-HPLC. The final product was obtained by freeze-drying and was purified and validated using RP-HPLC and MS (Fig. S1†).

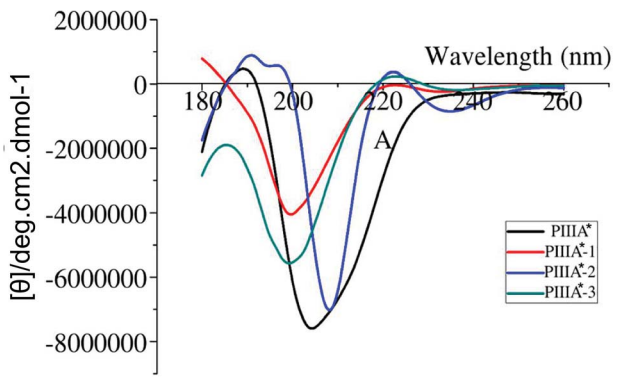

Fig. 2 The CD spectrum of PIIIA* and its analogues. The CD spectra of PIIIA*, PIIIA*-1, PIIIA*-2, and PIIIA*-3 are shown in black, red, blue and green, respectively.

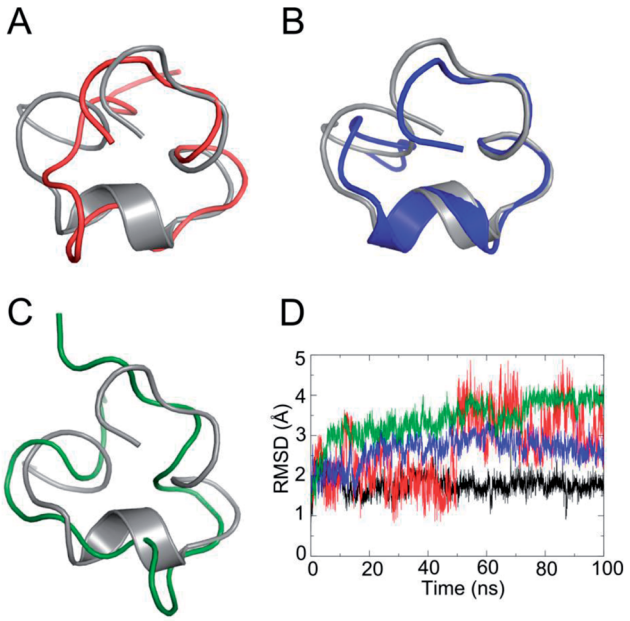

Fig. 3 Structure and stability comparison between PIIIA* and its disulfide deleted analogues. (A), (B), and (C) show the overlapped structures of PIIIA*-1, 2, and 3 with PIIIA*, respectively. Black represents PIIIA, and red, blue and green are PIIIA*-1, PIIIA*-2, and PIIIA*-3, respectively. (D) Shows an RMSD superposition diagram of PIIIA-1, 2, and 3. In (D) black, red, blue and green represent PIIIA*, PIIIA*-1, PIIIA*-2 and PIIIA*-3, respectively. The RMSD value was averaged for two MD trajectories.

3.2 Structural changes of PIIIA and its analogues

Deletion of the disulfide bond resulted in different CD spectra for PIIIA*-1, 2, and 3 (Fig. 2). In previous studies,[39,40] an α-helix structure exhibited a strong negative band around 208 nm, and a strong positive band around 190 nm. It was observed from the CD spectra (Fig. 2) that PIIIA* has strong negative and positive bands close to 208 and 190 nm, respectively, indicating that PIIIA* contains the α-helix component. Similarly, PIIIA*-2 strongly absorbs at 209 and 190 nm, and thus it was deduced that it contain an α-helix secondary structure. In addition, PIIIA*-2 has a negative absorption around 198 nm and a small and wide positive absorption at 220 nm indicating that PIIIA*-2 also contains part of a random coil.[39,40] In contrast, PIIIA*-1,3 only has a negative absorption at 198 nm and a small and wide positive absorption at 220 nm, indicating that most of the secondary structure of PIIIA*-1,3 is the random coil. Indeed, after the 100 ns MD simulation of PIIIA* and its analogues, we found that the structure of PIIIA*-1,3 contains a large number of random coils compared with PIIIA* (Fig. 3A and C). However, the structure of PIIIA*-2 is similar to that of PIIIA* and both contain an α-helix (Fig. 3B). This result is in line with our CD results. The α-helix in PIIIA*-2 enables a better stability than PIIIA*-1,3, which may lead to the inhibition activity of PIIIA*-2 being superior to that of PIIIA*-1,3. From the root mean square deviation (RMSD) analysis (Fig. 3D), the RMSD of PIIIA*-3 is greater than that of PIIIA*-1,2, suggesting that the conformation of PIIIA*-3 is the most significantly deviated from the initial conformation of the PIIIA* and its inhibitory activity is also the least active.

3.3 Electrophysiology

The biological activity of the four peptides (PIIIA*, PIIIA*-1, PIIIA*-2, and PIIIA*-3) on the hNa$_V$1.4 channels were measured by conventional patch clamp protocols. Control experiments were performed on the PIIIA* blocking to hNa$_V$1.4. Based on the percentage of blocking in a fixed peptide concentration, it was found that PIIIA*-2 had the best blocking effect on Na$_V$1.4 at three different concentrations among the three disulfides deleted analogues, but is still less potent than PIIIA* (Fig. 4A and B). At a concentration of 10 μM (Fig. 4B), PIIIA* exhibits a much stronger blocking effect on the hNa$_V$1.4 channel than

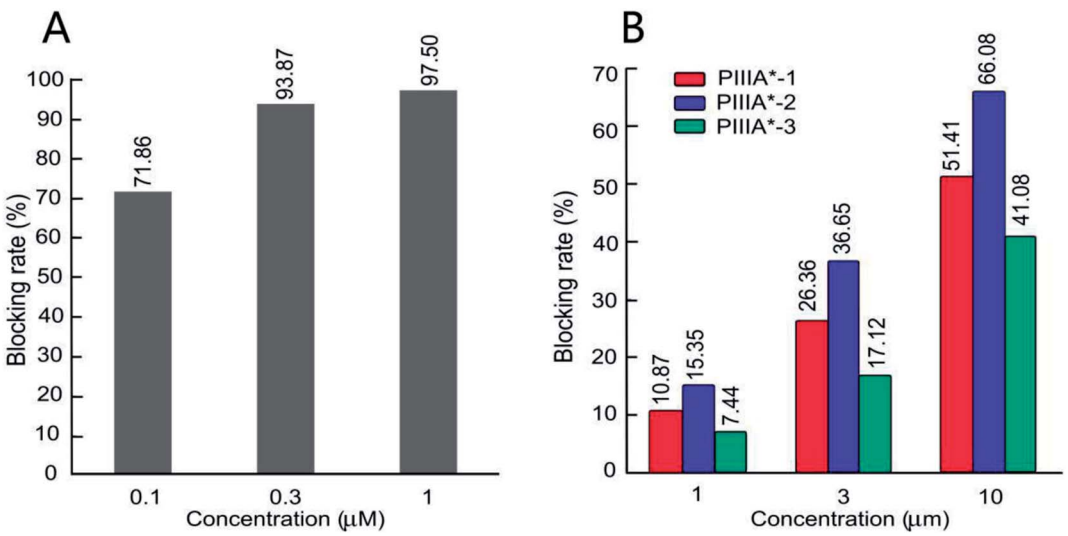

Fig. 4 Inhibition activity of the PIIIA* disulfide deleted analogues at Na$_V$1.4. (A) Represents the inhibition rate of PIIIA* on hNa$_V$1.4 at different concentrations. (B) The inhibition rate of PIIIA*-1, 2, and 3 on hNa$_V$1.4 at different concentrations.

Table 2 Interactions between the key amino acids on PIIIA-1, 2, 3 and $Na_V1.4$

Compounds	R12	R14	Q15	K17	O18	R20
PIIIA	E758,W761	F401,N404	L408	D1241	N404,D1533	D1541
PIIIA-1	W761	E755,E758	Q407	—	N404,D1533,N1536	D1541
PIIIA-2	W761	N404,E755	Q407	—	N404,D1533,N1536	N1536,D1541
PIIIA-3	—	N404,E755,E758	Q407	—	D1533,N1536	D1541

PIIIA*-1, PIIIA*-2, and PIIIA*-3. The current blocking rates for PIIIA*-1, PIIIA*-2 and PIIIA*-3 are 51.41%, 66.08%, and 41.08%, respectively. These results suggest that deletion of any one of the disulfide bonds significantly decreases the activity of PIIIA*. The inhibitory activity of PIIIA*-2 is stronger than PIIIA*-1, while PIIIA*-3 has the worst inhibitory activity, indicating that the varied disulfide bonds play different roles on the activity of PIIIA*, with the disulfide bond Cys11–Cys22 contributing most to the activity, and the disulfide bond Cys5–Cys21 contributing least to the activity. Indeed, related studies also showed that all of the three disulfides, especially Cys3–Cys6, were important for the inhibition of $Na_V1.4$ by GIIIA.[41] Deletion of any pair of disulfide bond could have an influence on the structure of the PIIIA and the GIIIA, and thus affect their inhibitory activity on the sodium channels. For BuIIIB, however, the Cys1–Cys4 bridge was more critical for $Na_V1.3$ blocking,[42] which indicates that the disulfide bond plays a different role in these three conotoxins. Exploring the effects of the disulfide bonds on the structure of PIIIA is particularly important to the rational design of PIIIA analogues.

3.4 Binding modes of $Na_V1.4$ with the PIIIA analogues

In order to determine the binding mode of PIIIA* at $Na_V1.4$, a 20 ns MD simulation was applied on a $Na_V1.4$/PIIIA*-1, 2, and 3 system, and each system was repeated five times. PIIIA is rich with positively charged residues, and is overall complementary to $Na_V1.4$, leading to the formation of numerous salt-bridges at the interface between PIIIA and $Na_V1.4$.[35] Previous mutagenesis data indicates that R12, R14, and R20 contribute most to the binding affinity of PIIIA to $Na_V1.4$.[43] Disulfide bond deletion affects the secondary structure of PIIIA*-1, 2, and 3, weakening their interaction with $Na_V1.4$. The R12 of PIIIA*-1, 2, and 3 only forms a very weak hydrogen bond interaction with W761, but the R12 of PIIIA forms salt-bridges with the E758 that is close to the pore filter.[35] Owing to the migration of R14, the R14 of PIIIA*-1, 2, and 3 forms salt-bridges with E755 that are weaker than that of PIIIA. As suggested by the results from the aforementioned electrophysiological testing, removal of the disulfide bond results in a significantly decreased binding affinity. In comparison with PIIIA*-1 and PIIIA*-3, the R20 of PIIIA-2 forms salt-bridges with D1541 at the periphery of the binding site, but the R20 of PIIIA*-1,3 is deflected, resulting in a deviation from D1541 and weakening of the salt-bridges. Therefore, the inhibition activity of PIIIA*-2 is stronger than PIIIA*-1 and PIIIA*-3. The results from the RMSD analysis (Fig. S3†) suggest that the three complexes reached equilibrium after a 20 ns MD simulation, with a RMSD of less than 1.2 Å, indicating that the $Na_V1.4$/PIIIA*-1, 2 and 3 systems were all relatively stable in MD.

3.5 Binding energy calculation and decomposition

In order to explore the effects of deletion of the disulfide bonds on the binding affinity of PIIIA* to the $Na_V1.4$ channel, we used MMGB/SA to calculate the energy contribution provided by both of these key residues of the binding site (Table 3) and the residues on PIIIA*-1, 2, and 3 (Fig. S3†). Meanwhile, the interaction between these key amino acids and $Na_V1.4$ were analyzed using the binding modes (Fig. 5). The binding energy calculations suggest that the binding energy of PIIIA*-2 to $Na_V1.4$ is lower than PIIIA*-1, 3 but that they are all much lower than PIIIA* (Table 3), which is consistent with the previously mentioned electrophysiological testing. It is indicated that deletion of the disulfide bond resulted in a significantly decreased affinity of PIIIA*. Mutagenesis studies show that the major residues that affect the interaction between PIIIA and $Na_V1.4$ channel are R12, R14, and R20.[43] Analyzing the energy contribution of these key residues in PIIIA*-1, 2, and 3, we found that the binding energy contributed by R20 of PIIIA*-1, 2 is much lower than PIIIA*-1, 3. This explains why PIIIA*-2 is better in comparison to PIIIA*-1 and PIIIA*-3. Compared with the contributions to the binding free energy of R12 of PIIIA*-1, 2, 3 (-0.61 kcal mol^{-1}, -0.49 kcal mol^{-1} and 0.02 kcal mol^{-1}, respectively), the R12 of PIIIA* is much lower, about

Table 3 The energy contribution of the key residues of the peptide

Residues	PIIIA*[a] (kcal mol^{-1})	PIIIA*-1[a] (kcal mol^{-1})	PIIIA*-2[a] (kcal mol^{-1})	PIIIA*-3[a] (kcal mol^{-1})
R12	−3.54(±0.966)	−0.61(±0.122)	−0.49(±0.244)	0.02(±0.175)
R14	−15.16(±0.812)	−11.83(±2.365)	−10.88(±0.435)	−12.94(±0.375)
R20	−7.46(±0.273)	−6.27(±1.254)	−8.46(±0.340)	−3.84(±0.544)
Total energy (kcal mol^{-1})	−51.06(±2.580)	−23.30(±1.093)	−25.02(±1.505)	−20.25(±1.607)

[a] The energy contribution was calculated using the MMGB/SA method and was averaged for five MD trajectories.

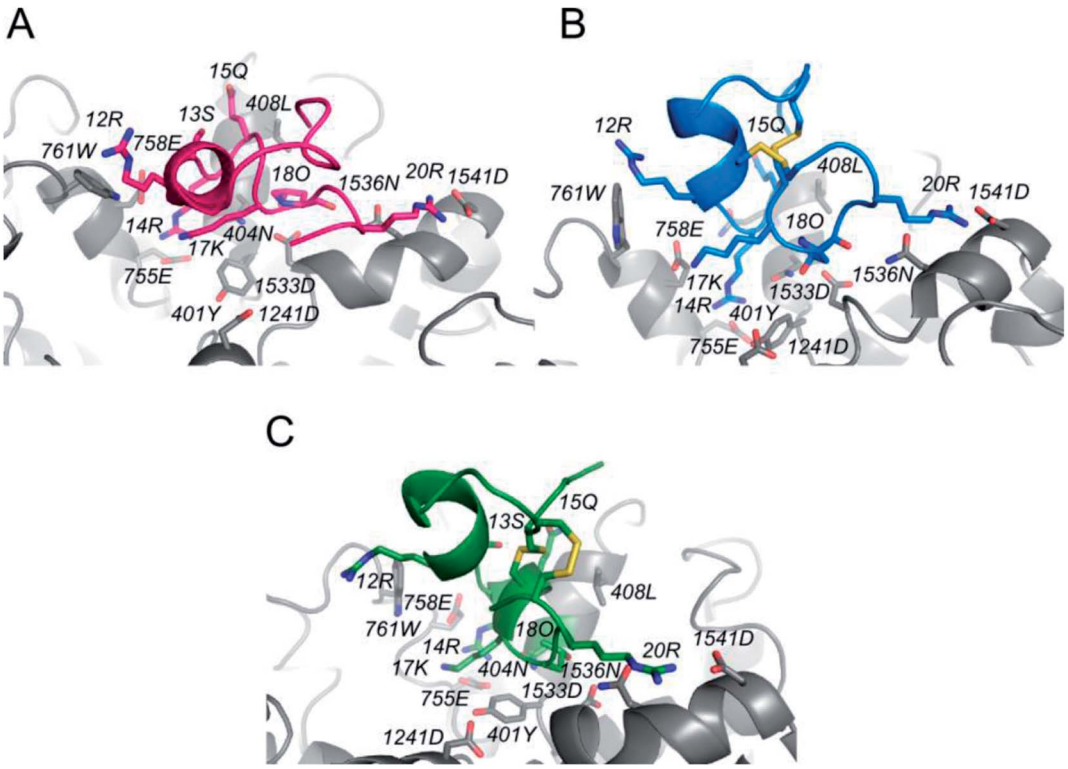

Fig. 5 The binding modes of $Na_V1.4$ with PIIIA and its analogues. (A), (B) and (C) represent the combination pattern of $Na_V1.4$/PIIIA*-1, $Na_V1.4$/PIIIA*-2, and $Na_V1.4$/PIIIA*-3, respectively. Red, blue and green represent PIIIA*-1, PIIIA*-2, and PIIIA*-3, respectively.

-3.54 kcal mol^{-1}. In addition, the binding free energy of the R14 of PIIIA* is lower than PIIIA*-1, 2, and 3. This further confirms that deletion of the disulfide bond results in the significantly decreased affinity of PIIIA*. More detailed pairwise interactions between PIIIA and $Na_V1.4$ are listed in Table 2.

4. Conclusions and perspectives

The purpose of this experiment was to explore the contribution of three pairs of disulfide bonds on the structure and inhibitory activity of PIIIA* from the aspects of experimental and computational modeling studies. Using the method of homology modeling and MD simulations, the inhibitory activity of PIIIA*-1, 2, and 3 was found to be significantly lower than for PIIIA*, which is in accordance with the experimental results obtaining using electrophysiological studies. By calculation of the binding energy and decomposition, we found that the second disulfide bond (Cys5–Cys21) had the minimum influence on the structure and activity of $Na_V1.4$, which is also in agreement with the results obtained from experimental studies. The blocking effects of PIIIA*-2 to $Na_V1.4$ is in the order of PIIIA*-2 > PIIIA*-3 > PIIIA*-1. The binding energy of $Na_V1.4$/PIIIA*-1, 2, and 3 also shows that the binding affinity of PIIIA*-2 on $Na_V1.4$ is better compared to PIIIA*-1, and 3 on $Na_V1.4$.

In conclusion, our study clearly shows that all three disulfide bonds in PIIIA are particularly important to maintaining the stability of the structure and to producing the effective inhibition of $Na_V1.4$. Furthermore, the results indicate that the second disulfide bond (Cys5–Cys21) connection has the smallest influence on the structure and activity of the peptide with $Na_V1.4$, followed by the first pair (Cys4–Cys6) and the third pair (Cys11–Cys22). The results from this study expand our knowledge of the importance of the three disulfide bonds in PIIIA, and will provide valuable information for the design of analogues with a better affinity and selectivity for therapeutic usage.

Conflicts of interest

There are no conflicts to declare.

Acknowledgements

This work was supported by the Fundamental Research Funds for the Central Universities (No. 201762011 for R. Y.), the National Natural Science of China (NSFC 81561148012), a grant from the National Natural Science Foundation of China (NSFC) (No. 81502977 for R. Y.), the National Laboratory Director fund (QNLM201709), the Scientific and Technological Innovation Project Financially Supported by the Qingdao National Laboratory for Marine Science and Technology (No. 2015ASKJ02) and the Taishan Scholars Program of Shandong, China.

Notes and references

1 H. Shen, Q. Zhou, X. Pan, Z. Li, J. Wu and N. Yan, *Science*, 2017, **355**, eaal4326.

2 M. Noda, T. Ikeda, H. Suzuki, H. Takeshima, T. Takahashi, M. Kuno and S. Numa, *Nature*, 1986, **322**, 826–828.
3 B. Rudy, *J. Physiol.*, 1978, **283**, 1–21.
4 G. P. Corpuz, R. B. Jacobsen, E. C. Jimenez, M. Watkins, C. Walker, C. Colledge, J. E. Garrett, O. Mcdougal, W. Li and W. R. Gray, *Biochemistry*, 2005, **44**, 8176.
5 R. B. Jacob and O. M. McDougal, *Cell. Mol. Life Sci.*, 2010, **67**, 17–27.
6 H. Terlau and B. M. Olivera, *Physiol. Rev.*, 2004, **84**, 41–68.
7 R. S. Norton, *Molecules*, 2010, **15**, 2825–2844.
8 K. J. Shon, B. M. Olivera, M. Watkins, R. B. Jacobsen, W. R. Gray, C. Z. Floresca, L. J. Cruz, D. R. Hillyard, A. Brink, H. Terlau and D. Yoshikami, *J. Neurosci.*, 1998, **18**, 4473–4481.
9 A. A. Tietze, D. Tietze, O. Ohlenschläger, E. Leipold, F. Ullrich, T. Kühl, A. Mischo, G. Buntkowsky, M. Görlach, S. H. Heinemann and D. Imhof, *Angew. Chem., Int. Ed. Engl.*, 2012, **51**, 4058–4061.
10 K. J. Shon, B. M. Olivera, M. Watkins, R. B. Jacobsen, W. R. Gray, C. Z. Floresca, L. J. Cruz, D. R. Hillyard, A. Brink, H. Terlau and D. Yoshikami, *J. Neurosci.*, 1998, **18**, 4473–4481.
11 P. Safo, T. Rosenbaum, A. Shcherbatko, D. Y. Choi, E. Han, J. J. Toledo-Aral, B. M. Olivera, P. Brehm and G. Mandel, *J. Neurosci.*, 2000, **20**, 76–80.
12 N. R. Munasinghe and M. J. Christie, *Toxins*, 2015, **7**, 5386–5407.
13 E. Leipold, F. Ullrich, M. Thiele, A. A. Tietze, H. Terlau, D. Imhof and S. H. Heinemann, *Biochem. Biophys. Res. Commun.*, 2016, **482**, 1135–1140.
14 P. Heimer, A. A. Tietze, C. A. Bäuml, A. Resemann, F. J. Mayer, D. Suckau, O. Ohlenschläger, D. Tietze and D. Imhof, *Anal. Chem.*, 2018, **90**, 3321–3327.
15 M. Góngora-Benítez, J. Tulla-Puche and F. Albericio, *Chem. Rev.*, 2014, **114**, 901–926.
16 T. S. Kang, Z. Radić, T. T. Talley, S. D. S. Jois, P. Taylor and R. M. Kini, *Biochemistry*, 2007, **46**, 3338–3355.
17 C. J. Armishaw, N. L. Daly, S. T. Nevin, D. J. Adams, D. J. Craik and P. F. Alewood, *J. Biol. Chem.*, 2006, **281**, 14136–14143.
18 P. Savarin, R. Romi-Lebrun, S. Zinn-Justin, B. Lebrun, T. Nakajima, B. Gilquin and A. Menez, *Protein Sci.*, 1999, **8**, 2672–2685.
19 Q. Zhu, S. Liang, L. Martin, S. Gasparini, A. Ménez and C. Vita, *Biochemistry*, 2002, **41**, 11488–11494.
20 M. Price-Carter, M. S. Hull and D. P. Goldenberg, *Biochemistry*, 1998, **37**, 9851–9861.
21 K. K. Khoo, Z.-P. Feng, B. J. Smith, M.-M. Zhang, D. Yoshikami, B. M. Olivera, G. Bulaj and R. S. Norton, *Biochemistry*, 2009, **48**, 1210–1219.
22 R. Yu, S. N. Kompella, D. J. Adams, D. J. Craik and Q. Kaas, *J. Med. Chem.*, 2013, **56**, 3557–3567.
23 R. Yu, S. N. Kompella, D. J. Adams, D. J. Craik and Q. Kaas, *J. Med. Chem.*, 2013, **56**, 3557–3567.
24 K. J. Nielsen, M. Watson, D. J. Adams, A. K. Hammarström, P. W. Gage, J. M. Hill, D. J. Craik, L. Thomas, D. Adams, P. F. Alewood and R. J. Lewis, *J. Biol. Chem.*, 2002, **277**, 27247–27255.
25 Y. Chen, F. H. Yu, E. M. Sharp, D. Beacham, T. Scheuer and W. A. Catterall, *Mol. Cell. Neurosci.*, 2008, **38**, 607–615.
26 Y. Chen, F. H. Yu, D. J. Surmeier, T. Scheuer and W. A. Catterall, *Neuron*, 2006, **49**, 409–420.
27 E. S. Bennett, *J. Membr. Biol.*, 2004, **197**, 155–168.
28 M. Chahine, P. B. Bennett, A. L. George and R. Horn, *Pflügers Arch.*, 1994, **427**, 136–142.
29 L. J. Cruz, W. R. Gray, B. M. Olivera, R. D. Zeikus, L. Kerr, D. Yoshikami and E. Moczydlowski, *J. Biol. Chem.*, 1985, **260**, 9280–9288.
30 K. Schroeder, B. Neagle, D. J. Trezise and J. Worley, *J. Biomol. Screening*, 2003, **8**, 50–64.
31 K. A. Young and J. H. Caldwell, *J. Physiol.*, 2005, **565**, 349–370.
32 A. Sali and T. L. Blundell, *J. Mol. Biol.*, 1993, **234**, 779–815.
33 N. Eswar, B. John, N. Mirkovic, A. Fiser, V. A. Ilyin, U. Pieper, A. C. Stuart, M. A. Marti-Renom, M. S. Madhusudhan, B. Yerkovich and A. Sali, *Nucleic Acids Res.*, 2003, **31**, 3375–3380.
34 R. Yu, D. J. Craik and Q. Kaas, *PLoS Comput. Biol.*, 2011, **7**, e1002011.
35 F. Chen, W. Huang, T. Jiang and R. Yu, *Mar. Drugs*, 2018, **16**(5), 153.
36 D. A. Case, D. S. Cerutti, T. E. Cheatham, III, T. A. Darden, R. E. Duke, T. J. Giese, H. Gohlke, A. W. Goetz, D. Greene, N. Homeyer, S. Izadi, A. Kovalenko, T. S. Lee, S. LeGrand, P. Li, C. Lin, J. Liu, T. Luchko, R. Luo, D. Mermelstein, K. M. Merz, G. Monard, H. Nguyen, I. Omelyan, A. Onufriev, F. Pan, R. Qi, D. R. Roe, A. Roitberg, C. Sagui, C. L. Simmerling, W. M. Botello-Smith, J. Swails, R. C. Walker, J. Wang, R. M. Wolf, X. Wu, L. Xiao, D. M. York and P. A. Kollman, *AMBER 2017*, University of California, San Francisco, CA, 2017.
37 R. Yu, Q. Kaas and D. J. Craik, *J. Phys. Chem. B*, 2012, **116**, 6097–6105.
38 K. Wittayanarakul, S. Hannongbua and M. Feig, *J. Comput. Chem.*, 2008, **29**, 673–685.
39 G. Holzwarth and P. Doty, *J. Am. Chem. Soc.*, 1965, **87**, 218–228.
40 N. J. Greenfield, *Nat. Protoc.*, 2006, **1**, 2876–2890.
41 P. Han, K. Wang, X. Dai, Y. Cao, S. Liu, H. Jiang, C. Fan, W. Wu and J. Chen, *Mar. Drugs*, 2016, **14**, 213.
42 B. R. Green, M.-M. Zhang, S. Chhabra, S. D. Robinson, M. J. Wilson, A. Redding, B. M. Olivera, D. Yoshikami, G. Bulaj and R. S. Norton, *FEBS J.*, 2014, **281**, 2885–2898.
43 J. R. McArthur, G. Singh, M. L. O'Mara, D. McMaster, V. Ostroumov, D. P. Tieleman and R. J. French, *Mol. Pharmacol.*, 2011, **80**, 219–227.